International Journal of Computational Mathematics and Scientific Computing

DOI: 10.5281/zenodo.21837677 | ISSN: 3141-643X | Volume: 1 | Issue: 2 | 2026

Characterization of Stable Regulatory Attractors in Malaria Parasite Gene Networks: Asynchronous Boolean Update Method

Abednego O. Isere[1*], Abraham O. Elakhe[2], Monday Okhuonurie[3]

[1,2,3]Department of Mathematics, Faculty of Physical Sciences, Ambrose Alli University, Ekpoma, 310001, Nigeria

[*]**Corresponding author:** isereao@aauekpoma.edu.ng

Abstract

Plasmodium falciparum, the most virulent human malaria parasite, possesses a highly regulated genome that supports survival, adaptation, virulence, drug resistance, developmental switching, and stress responses within the human host. This study characterizes stable regulatory attractors in a malaria-parasite gene regulatory network using an asynchronous Boolean update method. The network is formulated as a Boolean dynamical system with nine biological components: $X_1 = \mathrm{PfEMP1}$, $X_2 = \mathrm{PfCRT}$, $X_3 = \mathrm{PfMDR1}$, $X_4 = \mathrm{PfDHFR}$, $X_5 = \mathrm{AP2{-}G}$, $X_6 = \mathrm{PfSIR2A}$, $X_7 = \mathrm{PfK13}$, $X_8 = \mathrm{HP1}$, *and* $X_9 = \mathrm{H3K9me3}$*; these components represent regulators associated with virulence, drug resistance, developmental regulation, stress response, and epigenetic control. External pressure is represented by a general stress signal* ω *together with selectors for chloroquine (*λ*), antifolate pressure (*α*), artemisinin pressure (*β*), and partner-drug pressure (*ρ*). Fixed points are states satisfying* $F(X) = X$*; such states are invariant under either synchronous or asynchronous updating. Under the all-stress-OFF condition, the model yields three fixed points, whereas the all-stress-ON condition yields four fixed points. The attractors show how stress-dependent logical regulation can shift the network between distinct stable expression patterns and provide a mathematical framework for exploring regulatory states associated with parasite adaptation and antimalarial pressure.*

Keywords: *Plasmodium falciparum*; gene regulation; Boolean network; asynchronous update; fixed point; regulatory attractor.

1. Introduction

1.1. Background to the Study

Malaria is caused by unicellular parasites of the genus *Plasmodium* and is transmitted to humans by infected female *Anopheles* mosquitoes [29]. During its life cycle, the parasite differentiates through multiple developmental stages in the mosquito and human hosts [11, 23]. Following an infectious mosquito bite, sporozoites enter the bloodstream and invade hepatocytes. After liver-stage replication, merozoites are released and invade red blood cells. In *P. falciparum*, repeated erythrocytic cycles contribute to the clinical manifestations of malaria, including fever, anaemia, and severe disease [5, 25].

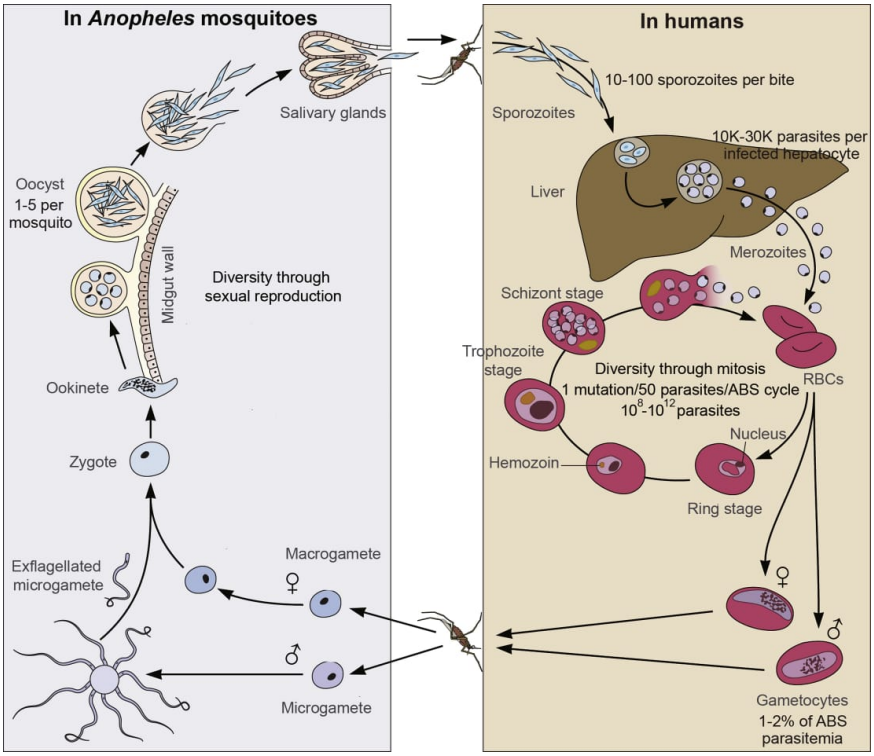

Figure 1: *Plasmodium falciparum* life-cycle diagram highlighting commonly studied stages. Source image reproduced from Serrano-Durán, López-Farfán, and Gómez-Díaz [26].

Experimental studies have provided extensive information about individual parasite genes and pathways, but stable biological states emerge from interactions among multiple regulators. Boolean network modelling offers a useful qualitative framework when regulatory relationships are known more reliably than their kinetic parameters. In a Boolean network, each component takes a binary state and changes according to a logical update function. This permits systematic analysis of fixed points, attractors, and state-transition structure [6, 22, 24].

Genetic and epigenetic variation in *P. falciparum* contributes to immune evasion, developmental switching, and antimalarial drug resistance [7, 26, 32]. Accordingly, a systems-level description of interactions among virulence-associated, resistance-associated, and epigenetic regulators can help clarify how different environmental or drug-pressure conditions are associated with stable network configurations. The present study therefore develops and analyzes an

asynchronous Boolean model for a nine-component regulatory network.

2. Preliminaries

2.1. Genes and Gene Expression

A gene is a hereditary unit encoded by a nucleotide sequence. Gene expression converts genetic information into functional RNA or protein products through transcription and, for protein-coding genes, translation and subsequent processing [13]. In *P. falciparum*, gene regulation is tightly linked to stage-specific development, host adaptation, immune evasion, and transmission [8, 26].

2.2. Boolean Networks

A Boolean network with n components is a discrete dynamical system on

$$\mathbb{F}_2^n = \{0,1\}^n,$$

where the state at time t is

$$X(t) = (X_1(t), X_2(t), \ldots, X_n(t)).$$

Each component has an update function

$$f_i : \mathbb{F}_2^n \longrightarrow \mathbb{F}_2,$$

and the full update map is

$$F(X) = (f_1(X), \ldots, f_n(X)).$$

The values 0 and 1 may be interpreted as inactive/active, absent/present, or low/high states, depending on the biological abstraction [6, 20].

2.3. Boolean Algebra and Square-Free Polynomial Representation

Over $\mathbb{F}_2$, Boolean operations can be represented algebraically by

$$A \wedge B = AB, \tag{1}$$
$$\neg A = 1 + A, \tag{2}$$
$$A \vee B = A + B + AB. \tag{3}$$

For three variables,

$$A \vee B \vee C = A + B + C + AB + AC + BC + ABC. \tag{4}$$

All arithmetic is modulo 2. Every Boolean function has a unique square-free polynomial representation in the quotient ring

$$\mathbb{F}_2[X_1, \ldots, X_n]/\langle X_1^2 - X_1, \ldots, X_n^2 - X_n \rangle,$$

so powers larger than one can be reduced using $X_i^2 = X_i$ [22].

2.4. Asynchronous Dynamics and Fixed Points

In an asynchronous Boolean system, one component is updated at a time. If component i is selected at time t, the successor state is

$$X_j(t+1) = \begin{cases} f_i(X(t)), & j = i, \\ X_j(t), & j \neq i. \end{cases}$$

The choice of updated component can be deterministic or nondeterministic, and therefore the asynchronous transition relation generally contains multiple possible successors from a given state [24, 6].

A fixed point is a state X^* satisfying

$$F(X^*) = X^*. \tag{5}$$

Because every component already equals its prescribed update at a fixed point, the state remains unchanged under any asynchronous update order. Thus, fixed points are schedule-independent even though non-fixed trajectories and basins of attraction can depend on the update scheme.

3. Model Formulation and Results

3.1. Variables

The model contains nine state variables. Table 1 summarizes the biological interpretation used in the manuscript.

Table 1: Core genes and regulatory components in the Boolean model.

Symbol	Full name	Modelled biological role
PfEMP1	*P. falciparum* erythrocyte membrane protein 1 (var-gene products)	Virulence, cytoadherence, and immune evasion
PfCRT	*P. falciparum* chloroquine resistance transporter	Chloroquine-resistance-associated component
PfMDR1	*P. falciparum* multidrug resistance protein 1	Multidrug-response/resistance-associated component
PfDHFR	*P. falciparum* dihydrofolate reductase	Antifolate-resistance-associated component
AP2-G	ApiAP2 transcription factor G	Gametocyte commitment and transmission regulation
PfSIR2A	*P. falciparum* silent information regulator 2A	Epigenetic regulation and var-gene silencing
PfK13	*P. falciparum* Kelch 13 protein	Artemisinin-resistance-associated component
HP1	Heterochromatin protein 1	Heterochromatin formation and transcriptional silencing
H3K9me3	Histone H3 lysine 9 trimethylation	Epigenetic repression and heterochromatic memory

The model uses NCBI gene annotations for several components and published literature on *P. falciparum* drug resistance and epigenetic regulation [14, 15, 16, 17, 18, 19, 7, 32].

3.2. External Stress and Drug Selectors

Four selector variables are used together with a general stress variable ω:

Table 2: External signals used in the model.

Symbol	Interpretation
ω	General host/drug stress signal
λ	Chloroquine-pressure selector
ρ	Partner-drug-pressure selector (e.g., amodiaquine, lumefantrine, or mefloquine)
α	Antifolate-pressure selector
β	Artemisinin-pressure selector

These selectors are mathematical switches rather than measured concentrations. The two extreme scenarios studied are all stress OFF,

$$\omega = 0, \qquad (\lambda, \alpha, \beta, \rho) = (0, 0, 0, 0),$$

and all stress ON,

$$\omega = 1, \qquad (\lambda, \alpha, \beta, \rho) = (1, 1, 1, 1).$$

3.3. Regulatory Interaction Diagram

Figure 2 summarizes the logical interactions encoded by the update rules. Arrows denote activating or maintaining influences and barred lines denote inhibitory influences.

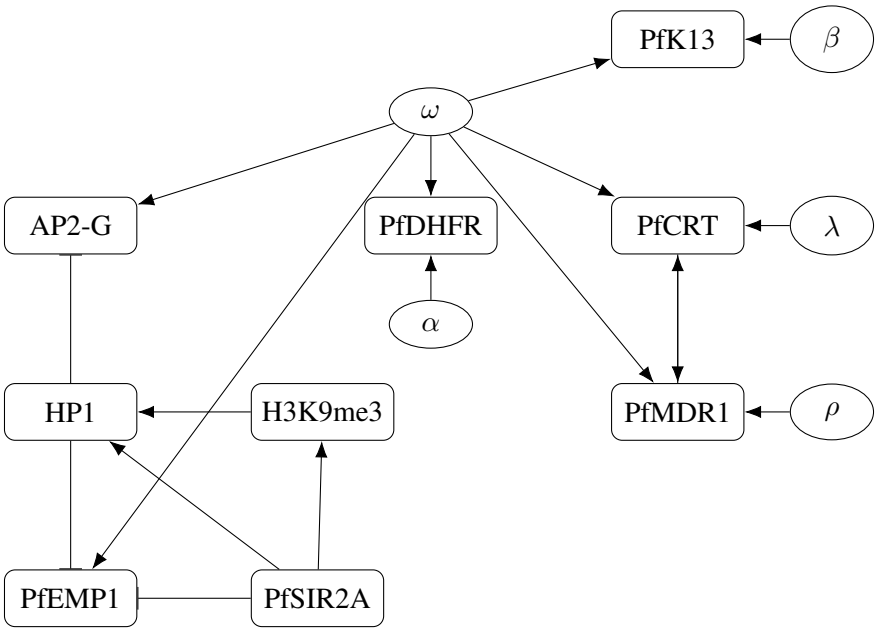

Figure 2: Schematic representation of the regulatory interactions encoded by the Boolean rules. The diagram is a cleaned reconstruction of the interaction concept in the source manuscript.

3.4. Boolean Update Rules

With all variables evaluated at time t unless otherwise indicated, the Boolean update rules are

$$\mathrm{PfEMP1}(t+1) = \neg\mathrm{HP1} \wedge \neg\mathrm{PfSIR2A} \wedge \omega, \tag{6}$$

$$\mathrm{PfCRT}(t+1) = [\mathrm{PfCRT} \wedge (\omega \wedge \lambda)] \vee [\mathrm{PfCRT} \wedge \mathrm{PfMDR1}], \tag{7}$$

$$\mathrm{PfMDR1}(t+1) = \mathrm{PfMDR1} \vee \mathrm{PfCRT} \vee (\omega \wedge \rho), \tag{8}$$

$$\mathrm{PfDHFR}(t+1) = \omega \wedge \alpha, \tag{9}$$

$$\mathrm{AP2\text{–}G}(t+1) = \neg\mathrm{HP1} \wedge \mathrm{AP2\text{–}G} \wedge \omega, \tag{10}$$

$$\mathrm{PfSIR2A}(t+1) = \neg\omega, \tag{11}$$

$$\mathrm{PfK13}(t+1) = \omega \wedge \beta, \tag{12}$$

$$\mathrm{HP1}(t+1) = \mathrm{H3K9me3} \wedge \mathrm{PfSIR2A}, \tag{13}$$

$$\mathrm{H3K9me3}(t+1) = \mathrm{PfSIR2A}. \tag{14}$$

For algebraic analysis, define

$$X_1 = \mathrm{PfEMP1}, \quad X_2 = \mathrm{PfCRT}, \quad X_3 = \mathrm{PfMDR1},$$
$$X_4 = \mathrm{PfDHFR}, \quad X_5 = \mathrm{AP2\text{–}G}, \quad X_6 = \mathrm{PfSIR2A},$$
$$X_7 = \mathrm{PfK13}, \quad X_8 = \mathrm{HP1}, \quad X_9 = \mathrm{H3K9me3}.$$

The square-free polynomial update functions over $\mathbb{F}_2$ are therefore

$$f_1 = (1 + X_8)(1 + X_6)\omega, \tag{15}$$
$$f_2 = X_2\omega\lambda + X_2X_3 + (X_2\omega\lambda)(X_2X_3), \tag{16}$$
$$f_3 = X_3 + X_2 + \omega\rho + X_2X_3 + X_3\omega\rho + X_2\omega\rho + X_2X_3\omega\rho, \tag{17}$$
$$f_4 = \omega\alpha, \tag{18}$$
$$f_5 = (1 + X_8)X_5\omega, \tag{19}$$
$$f_6 = 1 + \omega, \tag{20}$$
$$f_7 = \omega\beta, \tag{21}$$
$$f_8 = X_9X_6, \tag{22}$$
$$f_9 = X_6. \tag{23}$$

Equations (15)–(23) restore the terms that were visually lost in several equations of the source Word document and are algebraically equivalent to the stated Boolean rules.

3.5. Fixed Points Under All Stress OFF

There are $2^9 = 512$ possible states for the nine gene/regulator variables. Under

$$\omega = 0, \qquad \lambda = \alpha = \beta = \rho = 0,$$

the update functions simplify to

$$f_1 = 0, \quad f_2 = X_2X_3, \quad f_3 = X_3 \vee X_2,$$
$$f_4 = 0, \quad f_5 = 0, \quad f_6 = 1,$$
$$f_7 = 0, \quad f_8 = X_9X_6, \quad f_9 = X_6.$$

Solving $F(X) = X$ gives

$$X_1^{*(0)} = (0, 0, 0, 0, 0, 1, 0, 1, 1),$$
$$X_2^{*(0)} = (0, 0, 1, 0, 0, 1, 0, 1, 1),$$
$$X_3^{*(0)} = (0, 1, 1, 0, 0, 1, 0, 1, 1). \tag{24}$$

The common coordinates $X_6 = X_8 = X_9 = 1$ indicate that PfSIR2A, HP1, and H3K9me3 remain active in each OFF-state attractor, while PfCRT and PfMDR1 distinguish the three fixed points.

As a direct check, for $X = (0, 0, 0, 0, 0, 1, 0, 1, 1)$ every component satisfies $f_i(X) = X_i$. Hence an asynchronous update of any single component leaves the state unchanged.

3.6. Fixed Points Under All Stress ON

Under

$$\omega = 1, \qquad \lambda = \alpha = \beta = \rho = 1,$$

the fixed-point equations imply

$$X_1 = 1, \quad X_3 = 1, \quad X_4 = 1, \quad X_6 = 0, \quad X_7 = 1, \quad X_8 = 0, \quad X_9 = 0,$$

while X_2 and X_5 are free binary coordinates. Consequently, the four fixed points are

$$\begin{aligned} X_1^{*(1)} &= (1,0,1,1,0,0,1,0,0), \\ X_2^{*(1)} &= (1,0,1,1,1,0,1,0,0), \\ X_3^{*(1)} &= (1,1,1,1,0,0,1,0,0), \\ X_4^{*(1)} &= (1,1,1,1,1,0,1,0,0). \end{aligned} \tag{25}$$

Thus PfEMP1, PfMDR1, PfDHFR, and PfK13 are active in every all-stress-ON fixed point, whereas PfSIR2A, HP1, and H3K9me3 are inactive. PfCRT and AP2-G distinguish the four stable configurations.

For the illustrative initial state

$$(1,0,1,0,1,0,1,0,1),$$

a sequential asynchronous sweep changes the PfDHFR and H3K9me3 coordinates and reaches

$$(1,0,1,1,1,0,1,0,0),$$

which is the second fixed point in (25). Once this state is reached, every subsequent single-node update leaves it unchanged.

3.7. Asynchronous State-Transition Basins

The source computation generated basin diagrams for representative transitions into the fixed points. Figures 3 and 4 reproduce those computational outputs. In an asynchronous transition graph, edges correspond to admissible single-component updates; therefore, a non-fixed state may have several outgoing transitions, while a fixed point has only a self-invariant state.

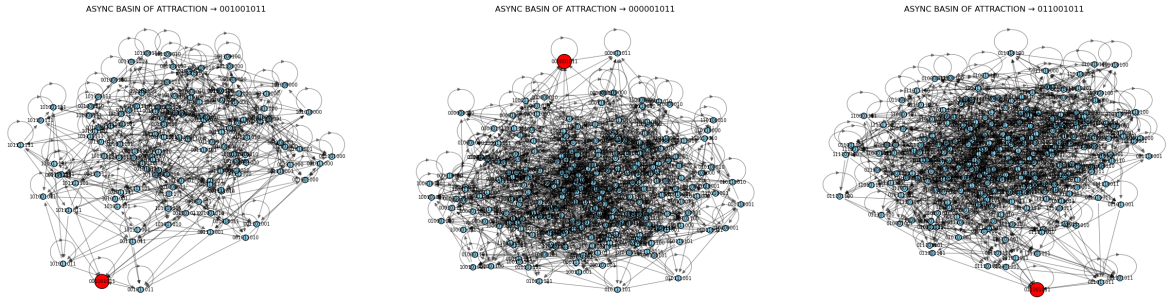

(a) 000001011 **(b)** 001001011 **(c)** 011001011

Figure 3: Asynchronous state-transition basin visualizations for the three all-stress-OFF fixed points.

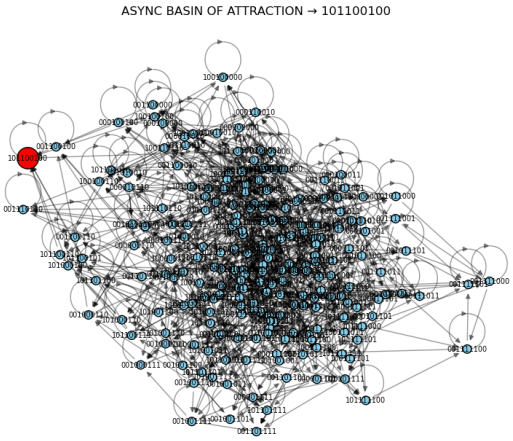

(a) 101100100

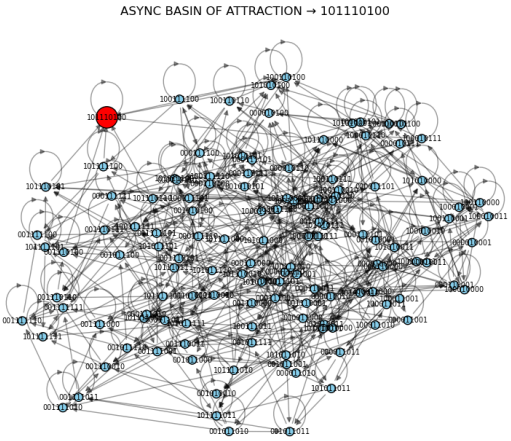

(b) 101110100

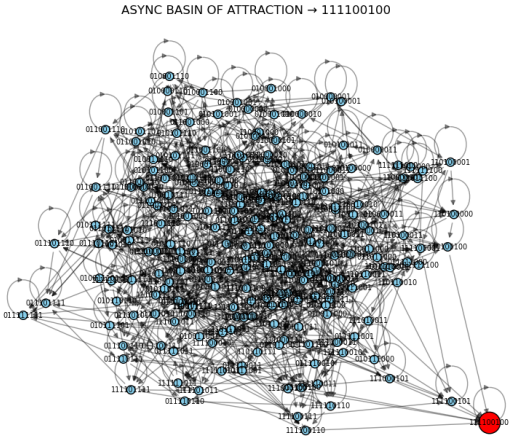

(c) 111100100

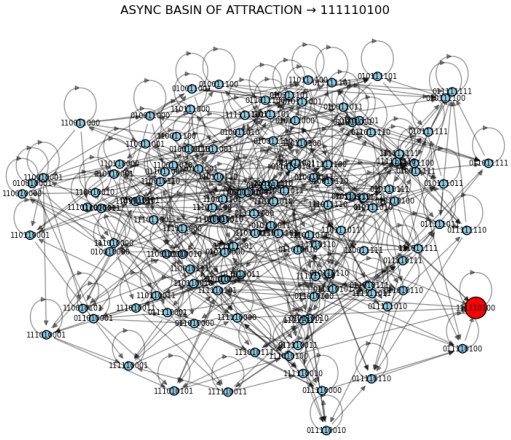

(d) 111110100

Figure 4: Asynchronous state-transition basin visualizations for the four all-stress-ON fixed points.

3.8. Fixed-Point Trajectories

A fixed-point trajectory is constant once the attractor is reached. The trajectory plots supplied in the source manuscript are reproduced in Figures 5 and 6. Overlapping binary traces can visually obscure one another because several components have identical 0/1 values throughout the plotted interval; this is a plotting effect rather than a change in the underlying state.

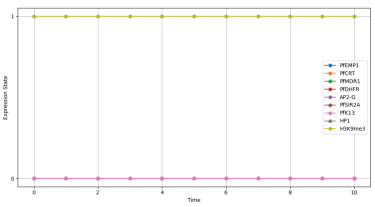

(a) OFF fixed point 1

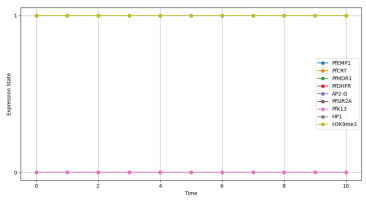

(b) OFF fixed point 2

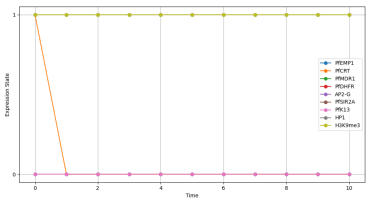

(c) OFF fixed point 3

Figure 5: Trajectory plots associated with the all-stress-OFF fixed points.

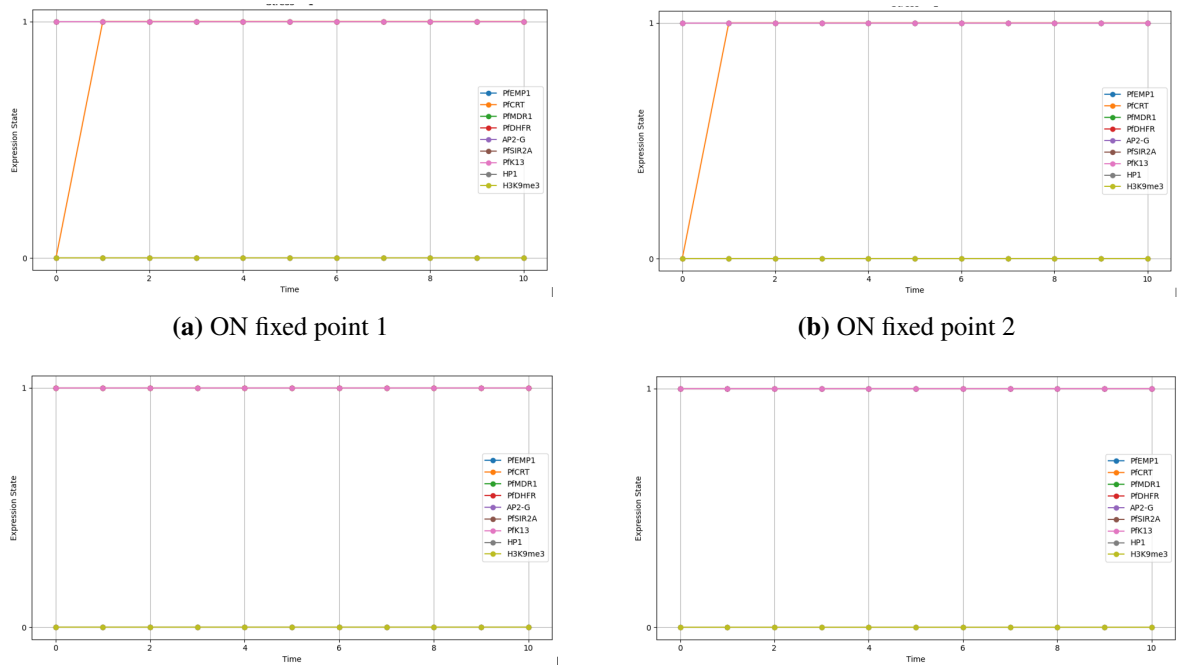

(a) ON fixed point 1

(b) ON fixed point 2

(c) ON fixed point 3

(d) ON fixed point 4

Figure 6: Trajectory plots associated with the all-stress-ON fixed points.

3.9. Fixed-Point Heatmaps

The heatmaps in Figure 7 compactly compare the attractor coordinates. For stress OFF, variability occurs in PfCRT and PfMDR1. For stress ON, variability occurs in PfCRT and AP2-G. The original manuscript incorrectly described the stress-ON heatmap as containing three fixed points; the displayed matrix and the derived solution (25) contain four.

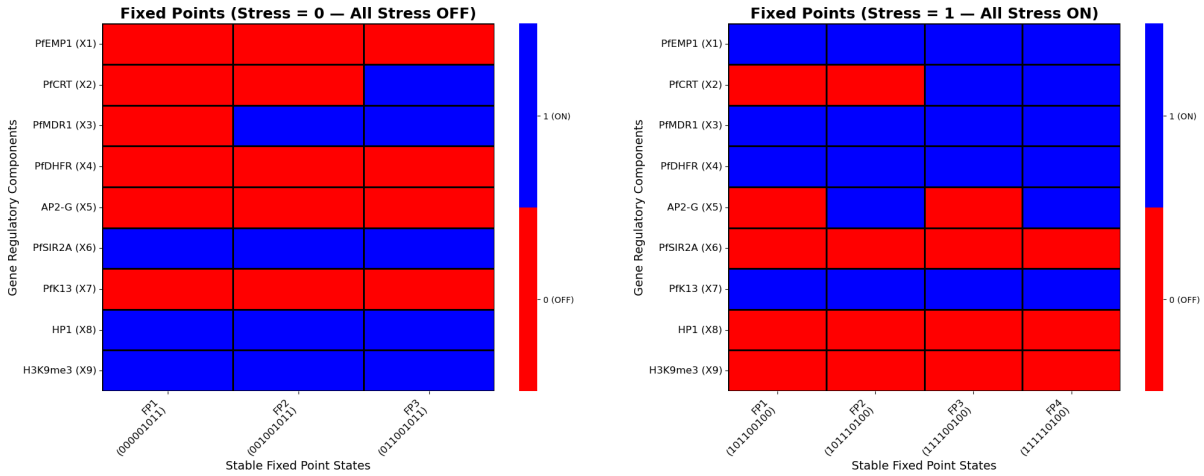

(a) All stress OFF

(b) All stress ON

Figure 7: Heatmaps of the stable fixed-point states.

4. Biological Interpretation of the Fixed Points

Under all stress OFF, the model produces three stable states in which PfSIR2A, HP1, and H3K9me3 are simultaneously active, while PfEMP1, PfDHFR, AP2-G, and PfK13 are inactive. The only variation occurs in PfCRT and PfMDR1. Within the assumptions of the Boolean rules, these attractors therefore represent multiple non-stressed regulatory configurations that share a common repressive/heterochromatic background.

Under all stress ON, the model produces four stable states with PfEMP1, PfMDR1, PfDHFR, and PfK13 active and PfSIR2A, HP1, and H3K9me3 inactive. PfCRT and AP2-G can independently take either binary value at a fixed point, creating four combinations. This transition is consistent with the logic encoded in the model: stress suppresses PfSIR2A through $f_6 = \neg\omega$, which in turn forces H3K9me3 and HP1 to zero through $f_9 = X_6$ and $f_8 = X_9X_6$; the loss of HP1/PfSIR2A repression allows the PfEMP1 rule to evaluate to one when $\omega = 1$. These interpretations are consequences of the chosen logical rules and should not be read as proof of direct causal biological mechanisms without experimental validation.

The model therefore provides a qualitative hypothesis-generating framework. It can be extended by incorporating experimentally measured regulatory edges, probabilistic update rules, stage-specific constraints, or perturbation analysis to test how deletion or inhibition of selected nodes changes the attractor landscape.

5. Conclusion

This study formulates a nine-component Boolean regulatory model for selected virulence-, resistance-, development-, and epigenetic-associated components of *Plasmodium falciparum*. The logical rules were converted into square-free polynomials over $\mathbb{F}_2$, and the fixed-point condition $F(X) = X$ was analyzed under two extreme stress regimes. Three fixed points occur when all stress selectors are OFF, whereas four occur when all selectors are ON. Because fixed points are invariant under every single-node update, these states are stable under asynchronous dynamics as well as under the full synchronous map.

The analysis demonstrates how a compact logical model can organize hypotheses about stable parasite regulatory configurations and how those configurations change when external stress switches are altered. The biological implications remain model-dependent, but the framework provides a tractable basis for subsequent refinement using experimental regulatory data, perturbation studies, and more detailed stochastic or multivalued models.

Funding

The authors received no specific funding for this work.

Conflict of Interest

The authors declare no conflict of interest.

Copyright and License

References

[1] Akerejola, R. F., Elakhe, O. A., & Isere, A. O. (2024). A non-standard finite difference discretization scheme applied to a malaria model. *African Journal of Mathematics and Statistics Studies, 7*(4), 226–247.

[2] Aleem, H. (2010). *An algebraic approach to modelling the regulation of gene expression* (Doctoral dissertation). University of Manchester.

[3] Ana, B., Daniel, S., Patrícia, A., Inês, S., & Verónica, M. (2023). Differential gene expression of malaria parasite in response to red blood cell-specific glycolytic intermediate 2,3-diphosphoglycerate (2,3-DPG). *International Journal of Molecular Sciences, 24*(23).

[4] Anja, R. J., Yvonne, A., & Lars, H. (2020). Cerebral *Plasmodium falciparum* malaria: The role of PfEMP1 in its pathogenesis and immunity, and PfEMP1-based vaccines to prevent it. *Immunological Reviews, 293*(1), 230–252. https://doi.org/10.1111/imr.12807

[5] Bakary, T., Boureima, S., & Sado, T. (2018). A mathematical model of malaria transmission in a periodic environment. *Journal of Biological Dynamics, 12*(1), 400–432. https://doi.org/10.1080/17513758.2018.1468935

[6] Cedric, L., & Remy, E. (2023). Boolean networks: Formalism, semantics, and complexity. In *Symbolic approaches to modeling and analysis of biological systems* (Chap. 5). https://doi.org/10.1002/9781394229086.ch5

[7] Cowell, A. N., & Winzeler, E. A. (2020). The genomic and genetic factors underlying drug resistance in malaria parasites. *The Lancet Infectious Diseases, 20*(10), e210–e220.

[8] Eliana, R., Virginia, M., Howick, V. M., Dahalan, F. A., W., K., C., J., et al. (2021). A single-cell atlas of *Plasmodium falciparum* transmission through the mosquito. *Nature Communications*. https://doi.org/10.1038/s41467-021-23434-z

[9] Isere, A. O., Osemwenkhae, J. E., & Okuonghae, D. (2014). Optimal control model for the outbreak of cholera in Nigeria. *African Journal of Mathematics and Computer Science Research, 7*(2), 24–30.

[10] Isere, A. O. (2024). A mathematical model of the effects of strike on Nigerian universities. *arXiv*. arXiv:2409.02945.

[11] Jaishree, T., Lei, Z., Sourav, S., Michal, S., & Zbynek, B. (2022). Stochastic expression of invasion genes in *Plasmodium falciparum* schizonts. *Nature Communications, 13*, 3004.

[12] Juilee, T. (2023). Pillars of biology: Boolean modeling of gene-regulatory networks. *Journal of Theoretical Biology, 578*, 111682.

[13] Lodish, H., Berk, A., Kaiser, C. A., et al. (2021). *Molecular cell biology* (9th ed.). W. H. Freeman.

[14] National Center for Biotechnology Information. (2024). *PF3D7_1328800 transcriptional regulatory protein sir2a [Plasmodium falciparum 3D7]*. NCBI Gene. https://www.ncbi.nlm.nih.gov/gene/814122

[15] National Center for Biotechnology Information. (2026a). *PF3D7_0523000 multidrug resistance protein 1 [Plasmodium falciparum 3D7]*. NCBI Gene. https://www.ncbi.nlm.nih.gov/gene/81304

[16] National Center for Biotechnology Information. (2026b). *PF3D7_0709000 chloroquine resistance transporter [Plasmodium falciparum 3D7]*. NCBI Gene. https://www.ncbi.nlm.nih.gov/gene/2655199

[17] National Center for Biotechnology Information. (2026c). *PF3D7_0417200 bifunctional dihydrofolate reductase-thymidylate synthase [Plasmodium falciparum 3D7]*. NCBI Gene. https://www.ncbi.nlm.nih.gov/gene/9221804

[18] National Center for Biotechnology Information. (2026d). *PF3D7_1222600 AP2 domain transcription factor AP2-G [Plasmodium falciparum 3D7]*. NCBI Gene. https://www.ncbi.nlm.nih.gov/gene/811269

[19] National Center for Biotechnology Information. (2026e). *PF3D7_1343700 kelch protein K13 [Plasmodium falciparum 3D7]*. NCBI Gene. https://www.ncbi.nlm.nih.gov/gene/814205

[20] Nezamuldeen, L., & Jafri, M. S. (2024). Boolean modeling of biological network applied to protein-protein interaction network of autism patients. *Biology, 13*(8), 606. https://doi.org/10.3390/biology13080606

[21] Papatheodorou, I., Moreno, P., Manning, J., Fuentes, A. M., George, N., Fexova, S., et al. (2020). Expression Atlas update: From tissues to single cells. *Nucleic Acids Research, 48*(D1), D77–D83. https://doi.org/10.1093/nar/gkz947

[22] Raina, R., & Macauley, M. (2019). *Algebraic and computational biology*. Mathematics in Science and Engineering.

[23] Rajneesh, Tiwari, R., Singh, V. K., Kumar, A., Gupta, R. P., Singh, A. K., Gautam, V., & Kumar, R. (2023). Advancements and challenges in developing malaria vaccines: Targeting multiple stages of the parasite life cycle. *ACS Infectious Diseases, 9*, 1795–1814. https://doi.org/10.1021/acsinfecdis.3c00332

[24] Roberto, B., Roberta, G., Paolo, M., & Lucia, N. (2020). A survey of gene regulatory networks modelling methods: From differential equations to Boolean and qualitative bioinspired models. *Journal of Membrane Computing, 2*, 207–226.

[25] Santos, J. M., Josling, G. A., & Ross, P. (2020). Red blood cell invasion by the malaria parasite *Plasmodium falciparum*: Structural basis for regulation of ligand-receptor interactions. *PLoS Pathogens, 16*(10), e1008899.

[26] Serrano-Durán, R., López-Farfán, D., & Gómez-Díaz, E. (2022). Epigenetic and epitranscriptomic gene regulation in *Plasmodium falciparum* and how we can use it against malaria. *Genes, 13*(10), 1734. https://doi.org/10.3390/genes13101734

[27] Sibomana, O., Bukuru, J., Saka, S. A., Uwizeyimana, M. G., Kihunyu, A. M., Obianke, A., et al. (2025). Routine malaria vaccination in Africa: A step toward malaria eradication? *Malaria Journal, 24*, 1. https://doi.org/10.1186/s12936-024-05235-z

[28] Walker, A., Ross, A., & Nsanzabana, C. (2025). Changes in the prevalence of antimalarial partner drug resistance markers and policy in 6 Sub-Saharan African countries from 2000 to 2021: A systematic review. *Open Forum Infectious Diseases, 12*(9), ofaf508. https://doi.org/10.1093/ofid/ofaf508

[29] World Health Organization. (2022). *World malaria report 2022*. World Health Organization.

[30] World Health Organization. (2024). *Strategy to respond to antimalarial drug resistance in Africa*. World Health Organization.

[31] World Health Organization. (2025). *Question and answer: Artemisinin partial resistance*. World Health Organization.

[32] Zhang, Q., & Scherf, A. (2021). Antigenic variation in *Plasmodium falciparum* malaria. *Annual Review of Microbiology, 75*, 737–761.